

**FORECASTING ELECTRICITY GENERATION
FROM RENEWABLE SOURCES IN DEVELOPING COUNTRIES
(ON THE EXAMPLE OF UKRAINE)**

Ihor Miroshnichenko

Kyiv National Economic University named after Vadym Hetman
54/1 Peremogy Ave., Kyiv, 03057, Ukraine
ORCID: 0000-0002-1307-7889, E-mail: ihor.miroshnichenko@kneu.ua

Tetiana Kravchenko

Kyiv National Economic University named after Vadym Hetman
54/1 Peremogy Ave., Kyiv, 03057, Ukraine
ORCID: 0000-0002-1506-3595, E-mail: ktv19@ukr.net

Yuliia Drobyna

Energy Trade Group LLC
6 Ivana Mazepa Str., Kyiv, 01010, Ukraine
E-mail: drobyna.yuliia@gmail.com

Electricity generation forecasting is a common task that helps power generating companies plan capacity, minimize costs, and detect anomaly. Despite its importance, there are serious challenges associated with obtaining reliable and high-quality forecasts, especially when it comes to the newly created renewable electricity market.

A practical approach to predicting the generation of electricity from alternative sources in developing countries (on the example of Ukraine) based on the use of classical (ARIMA, TBATS) and modern (Prophet, NNAR) approaches is proposed.

The legal framework regulating the process of Ukraine's entry into the pan-European energy market and its functioning was analyzed: the weak points of the legislation on responsibility, the permissible accuracy of weather conditions data, and the lack of data on the monitoring infrastructure are indicated.

Among all the proposed alternatives, the Prophet model was the most accurate, since it allows you to simultaneously take into account several seasonalities (hourly, daily, weekly, monthly, and holidays). According to this, for an operational forecast (6 hours) the best model is the one that takes into account hourly seasonality, and for short-term forecasts (24 and 48 hours) and medium-term forecast (72 hours) the most accurate models are those taking into account hourly, daily, weekly seasonality and weather conditions.

The obtained forecasts and model quality indicators approve the feasibility of applying the proposed approach and the constructed models that can be used in a wide range of economic problems.

Keywords: *alternative energy, forecasting, Prophet model, neural network autoregression*

JEL Classification: C6, C45, C8, Q42, Q47

Introduction

The use of alternative energy is one of the promising area of energy development, which is caused by several factors. The main among them are avoiding energy instability, which is caused by the energy crises due to dependence on energy imports, the reduction of harmful emissions, the need to preserve non-renewable energy sources. A new electricity market has recently been started to operate in Ukraine, the purpose of which is to introduce competitive mechanisms for the electricity market functioning, ensure the free choice of counterparties and the consumer's right to freely choose an electricity supplier.

On April 13, 2017, the Verkhovna Rada of Ukraine passed the Law of Ukraine "On Electricity Market" [1]. Law passing became a precondition for important structural changes in the electricity sector of Ukraine, such as, for example, the modernization of the industry, the integration of the electricity market of Ukraine into regional energy markets and the development of the process of entering into the pan-European energy market. As a result, a new electricity market started to operate on July 1, 2019.

In addition, legal framework includes the following: the Laws of Ukraine "On Alternative Energy Sources" [2], "On Combined Heat and Power (Cogeneration) and Waste Energy Potential" [3], "On National Commission for State Regulation of Energy and Utilities" [4], "On Natural Monopolies" [5], "On Protection of Economic Competition" [6], "On Environmental Protection" [7], international agreements and other legal acts of Ukraine. According to the legislation, now each enterprise is obliged to submit predicted values of electricity consumption and fines are provided for non-compliance with these rules. A detailed study of the legislation shows the need to build short-term forecasts electricity generation.

Analysis of recent research and publications

The task of forecasting electricity generation is quite popular [8-10], but the ways to solve it quite often depend on the specifics of the market, geography, climate and other socio-economic factors.

Among scientific research there are a number of approaches to forecasting the generation of electricity. Paper [11] presents an exhaustive review and categorization of data processing in wind energy forecasting. The utilized techniques are classified into seven categories according to the applications: decomposition, feature selection, feature extraction, denoising, residual error modeling, outlier detection, and filter-based correction. However, all the presented approaches are mainly aimed at forecasting wind energy, which may differ from other types of energy, especially in a new market. Paper [12] present a comprehensive review of decomposition-based wind forecasting methods in order to explore their effectiveness.

The article [13] mainly focuses on predicting based on several classes of solar energy models: persistence, classical statistics, machine learning, cloud-motion tracking, numerical weather prediction and hybrid models. Machine learning and hybrid models have the best performance for intra-hour performance in all climates. The best intra-hour forecasts are provided in all climates by machine learning and classical statistics models while the hybrid models perform well in tropical and snow climates. For day-ahead forecasts the hybrid models have shown very good performance in all climates. It is concluded that hybrid models tend to have better performance.

The article [14] gives a broad literature survey of the intelligent predictors in the field of wind energy forecasting, including four types of shallow predictors (artificial neural network, extreme learning machine, support vector machine, and fuzzy logic model) and four types of deep learning-based predictors (autoencoder, restricted Boltzmann machine, convolutional neural network, and recurrent neural network). However, the paper is of a theoretical nature, without solving applied problems.

More and more works are devoted to the use of neural networks in building short-term forecasts by electricity market participants. Thus, the paper [15] reviewed recent developments in the field of probabilistic, multivariate, and multihorizon time series forecasting and empirically evaluate the performance of novel global deep learning models for forecasting wind and solar generation, electricity load, and wholesale electricity price for intraday and day-ahead time horizons. The paper [16] proposes an artificial neural network to predict the solar energy generation produced by photovoltaic

generators. However, the article does not consider alternative models that are less demanding on the capacity of information systems and give no less accurate forecasts.

In paper [17] a hybrid ensemble deep learning framework is proposed to forecast short-term photovoltaic power generation in a time series manner. The forecasting results are flattened and combined with a fully connected layer to enhance forecasting accuracy. Particular attention is paid to assessing the effectiveness of models for short-term forecasting (from 7.5 to 60 minutes). The results were compared with alternative methods, including the persistent model, the auto-regressive integrated moving average model with exogenous variable, multi-layer perceptron, and the long short-term memory neural networks in *MAPE*, *RMSE*, *MAE* metrics. However, for a short-term forecasting problem with a longer forecasting horizon, the presented approach can show completely different results.

To summarize the analysis of modern research, there is a certain trend towards the use of neural networks to solve the problem of predicting energy generation, as well as the use ensemble models, which often increases the efficiency of obtaining results. At the same time, it becomes obvious that energy forecasting requires an individual approach for its solution, and the effectiveness of models often depends on the requirements of the legislation of each individual country, the specifics of the market, and the availability of sufficient and diverse information.

Purpose

There is a need for research and analysis of the energy sector and its processes in order to identify possible obstacles and develop practical recommendations for their solution. In addition, an important requirement is to provide the forecasting of renewable energy generation, that helps governments and organizations with capacity planning, target setting and anomaly detection.

Materials and Methods

On August 18, 2017, the Cabinet of Ministers of Ukraine adopted the Order “On approval of the Energy Strategy of Ukraine up to 2035” [18], which identifies 3 stages of implementation:

- in the first phase, by 2020, it is expected an effective progress in the field of renewable energy sources by increasing their share in final consumption to 11% (or 8% of total primary energy supply) through a stable and predictable policy in the field of stimulating the development of renewable energy sources and in the field of attracting investments;

- in the second phase, by 2025, there should be intensive investment in the renewable energy sector, the development of distributed generation, in particular the goal is to develop and implement a plan for the implementation of “smart” energy networks (Smart Grids) and further creation of an extensive infrastructure for the development of electric transport;

- in the third phase, by 2035, it is assumed that renewable energy will develop at the most dynamic pace compared to other types of electricity production, which will increase their share in the structure of total primary energy supply to 25%.

More precise indicators that should be achieved as a result of the implementation of the Energy Strategy are shown in Table 1.

Table 1

**KEY PERFORMANCE INDICATORS
OF THE ENERGY STRATEGY OF UKRAINE UP TO 2035**

Key performance indicator	Type	2015	2020	2025	2030	2035
Share of renewable energy (including hydrogenerating capacity and thermal energy) in the total primary energy supply, %	Target	4%	8%	12%	17%	25%
Share of renewable energy (including hydrogenerating capacity) in electricity generation, %	Target	5%	7%	10%	>13%	>25%
CO ₂ emissions to the 1990 level	Limit	–	<60%	<60%	<60%	<50%
Reduction of CO ₂ emissions eq. on final fuel consumption, % from 2010	Target	–	>5	>10	>15	>20
Share of capacity in thermal generation that meets EU environmental requirements (SO ₂ , NO _x emissions, ash), %	Target	<1%	<10%	<40%	85%	100%

Among the main measures to achieve the targets and key performance indicators planned to be implemented in the renewable energy sector, the following are identified (according to [18]):

- implementation of a stable and predictable policy to stimulate the construction of solar and wind power plants;
- conducting international communication events to encourage international strategic and financial investors to enter the renewable energy market of Ukraine;
- construction and commissioning of 5 GW of renewable energy capacity (except for high-capacity hydropower plants);
- incentives for the use of biomass in the generation of electricity and heat, as a fuel in enterprises where biomass is a residual product; informing about the possibilities of using biomass as a fuel in the individual heat supply; promoting the creation of conditions for the formation of competitive biomass markets.

The study of alternative energy development in Ukraine encourages to analyze the current state of the electricity market as a whole. The official website of the National Power Company Ukrenergo publishes data about the functioning of the Integrated Power System (IPS), electricity generation and consumption balance, installed capacity of the IPS of Ukraine, electricity consumption forecasts by areas of regulation, etc. [19]. Fig. 1, built on these data, shows the capacity of the components of generation of the IPS of Ukraine for the period December 2010 – October 2019.

Fig. 1 shows that there was a significant decrease in the capacity of solar and wind power plants at the end of 2015 compared to the same period in 2014. The reason is the armed aggression against Ukraine, that is why values do not include the temporarily occupied territories of Ukraine (certain districts of Donetsk and Luhansk regions and Crimea), where large amount of renewable energy sources was located, especially wind power plants. Another important aspect of the development of alternative energy sources was the introduction of biofuel plants in 2014.

At the end of 2015 the installed capacity of the IPS of Ukraine was 50883.40 MW (according to Fig. 1), 27.19% of which belonged to nuclear power plants (NPP), 48.19% – thermal power plants (TPP), 11.67% – combined heat and power (CHP), 9.23% – hydro power plants (HPP), 2.33% – pumped storage power plants (HPSPP), 0.71% – solar power plants (SPP), 0.57% – wind power plants (WPP), 0.1% – biofuel plants (Fig. 2).

As of the 1st	Components of generation									In general MW
	NPP MW	TPP MW	CHP MW	HPP MW	HPSPP MW	SPP MW	WPP MW	Biofuel plants MW		
12/2010	18315	27347	6426.9	4396.9	861.5	8.1	86.2	0	53 161.60	
12/2011	18315	27272	6429.8	4603.5	861.5	187.5	121.3	0	53 310.60	
12/2012	18315	27408	6482.4	4609.7	861.5	317.8	262.8	0	53 777.60	
12/2013	18315	27616	6646.2	4610.6	861.5	563.4	371.7	0	54 504.46	
12/2014	18315	27700	6599.3	4668.2	1385.5	582	508.7	35.4	55 114.10	
12/2015	18315	24523	5940.4	4698.5	1385.5	359.1	289.5	52.4	50 883.40	
12/2016	18315	24585	5946.8	4711	1509.5	457.97	300.4	62.6	51 388.27	
12/2017	18315	24585	5972.3	4719.2	1509.5	758.4	338.4	96.9	51 784.70	
1/2018	18315	24585	5987.1	4719.2	1509.5	767.2	368.6	97.3	51 848.90	
2/2018	18315	24585	5987.1	4719.2	1509.5	771.94	368.6	97.7	51 854.04	
3/2018	18315	24598	5979.1	4729.8	1509.5	802.9	371.8	97.7	51 925.80	
4/2018	18315	24598	6015.3	4729.9	1509.5	805.8	374.9	97.7	51 966.10	
5/2018	18315	24598	6015.3	4729.9	1509.5	809	374.9	97.7	51 969.30	
6/2018	18315	24598	6015.3	4729.9	1509.5	856.4	374.9	97.7	52 016.70	
7/2018	18315	24603	6014.7	4729.9	1509.5	937.4	378.1	98.3	52 105.90	
8/2018	18315	24603	6014.7	4730.2	1509.5	1003.7	379.46	98.7	52 174.26	
9/2018	18315	24618	6014.7	4730.2	1509.5	1039.6	379.46	98.7	52 225.16	
10/2018	18315	21842	6014.7	4730.4	1509.5	1083.7	386.5	98.7	49 500.50	
11/2018	18315	21842	6014.7	4731.4	1509.5	1184.2	386.5	98.7	49 602.00	
12/2018	18315	21842	6099.5	4731.7	1509.5	1224.8	389	98.7	49 730.20	
1/2019	18315	21842	6099.5	4731.7	1509.5	1310.4	389	98.8	49 815.90	
2/2019	18315	21842	6099.5	4732.4	1509.5	1629.8	441.3	101	50 190.30	
3/2019	18315	21842	6099.5	4732.4	1509.5	1692.1	510.6	101	50 322.10	
4/2019	18315	21842	6099.5	4732.4	1509.5	1777.8	579.5	102.8	50 478.50	
5/2019	18315	21842	6099.5	4732.4	1509.5	1925.4	611.9	102.8	50 658.50	
6/2019	18315	21842	6099.5	4732.4	1509.5	2161.6	611.9	102.5	50 897.20	
7/2019	18315	21842	6099.5	4818.5	1474.4	2312.4	628.6	106.5	51 116.90	
8/2019	18315	21842	6099.5	4818.7	1474.4	2271.2	636.6	107.1	51 184.50	
9/2019	18315	21842	6099.5	4818.7	1474.4	2514.8	697.9	108.3	51 390.60	
10/2019	18315	21842	6099.5	4819.3	1474.4	3038.1	831.7	115.7	52 055.80	

Fig. 1. Capacity of the components of generation of the Integrated Power System of Ukraine for the period 2010–2019

The capacity of renewable energy (RE) equipment was 701.00 MW, 51.23% of which belonged to SPP, 41.30% – WPP, 7.48% – biofuel plants (Fig. 3).

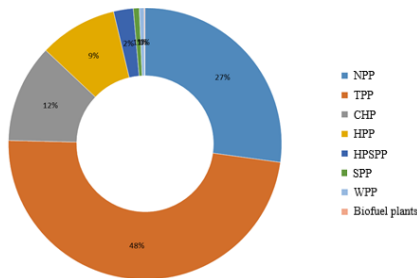


Fig. 2. Installed capacity of the IPS of Ukraine in percentage values as at December 2015

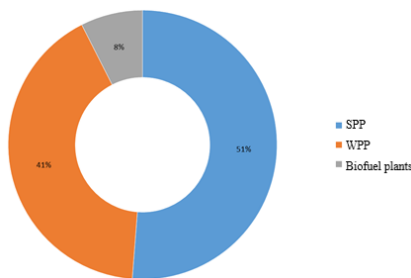


Fig. 3. Capacity of RE equipment of Ukraine in percentage values as at December 2015

As at October 2019 the installed capacity of the IPS of Ukraine was 52055.80 MW, 26.58% of which belonged to NPP, 41.96% – TPP, 11.72% – CHP, 9.26% – HPP, 2.83% – HPSPP, 5.84% – SPP,

1.6% – WPP, 0.2% – biofuel plants (Fig. 4). The capacity of RE equipment was 3985.60 MW, 76.23% of which belonged to SPP, 20.87% – WPP, 2.90% – biofuel plants (Fig. 5).

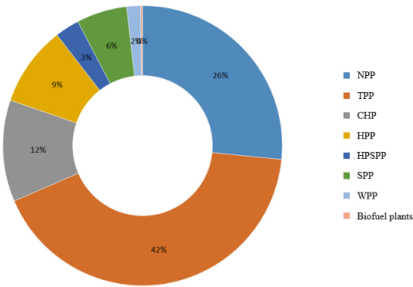


Fig. 4. Installed capacity of the IPS of Ukraine in percentage values as at October 2019

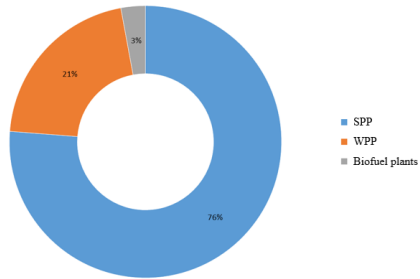


Fig. 5. Capacity of RE equipment of Ukraine in percentage values as at October 2019

An analysis for the period 2015-2019 showed that the installed capacity of RE increased, namely SPP 8.46 times (in 2015 – 359.1 MW, in 2019 – 3038.2 MW), WPP 2.87 times (in 2015 – 289.5 MW, in 2019 – 831.7 MW), biofuel stations 2.2 times (in 2015 – 52.4 MW, in 2019 – 115.7 MW). In general, during this period, the capacity of RE equipment increased by 6.28% (in 2015 – 1.38%, in 2019 – 7.66%). The share of SPP equipment capacity increased by 25% for the same period, while the share of WPP capacity and biofuel plants decreased by 20.43% and 4.57%, respectively.

Thus, the trend towards developing the capacity of renewable energy continues, and most attention is focused on the development of solar power plants. However, this development takes place through the reduction / replacement of TPP capacity. Fig. 1 shows that the capacity of TPP decreased by 2681 MW, in percentage by 6.2%, respectively (in 2015 the share of TPP in the total capacity of IPS of Ukraine was 48.2%, in October 2019 – 42%).

Detailed hourly data of generating components NPP, CHP, RE, TPP, HPP and HPSPP from 01.01.2016 to 31.10.2019 are presented in Figs. 6-10, respectively. The graphs show that there is the seasonality of NPP and CHP generation. In 2019, there was a clear increase in the RE generation of electricity, because of new SPP and WPP, which had recently been built and joined the IPS of Ukraine.

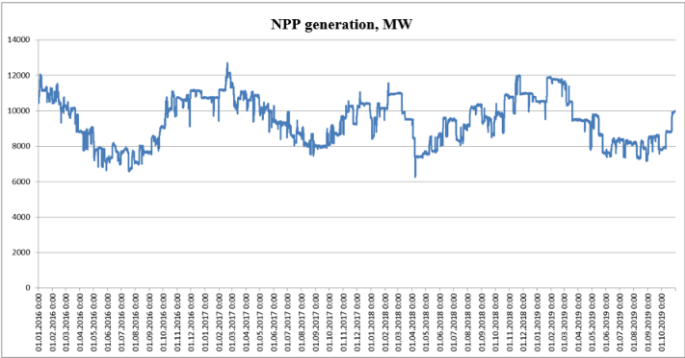


Fig. 6. Hourly data of NPP generation from 01.01.2016 to 31.10.2019

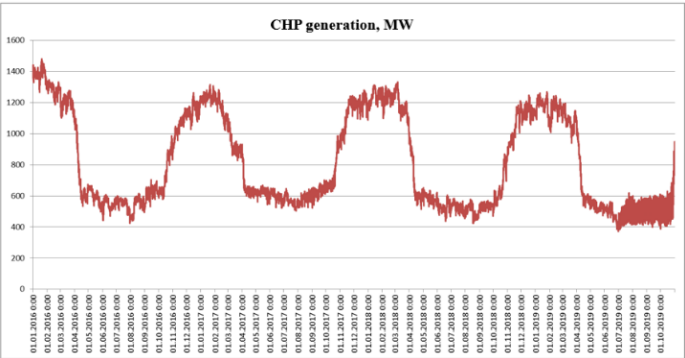


Fig. 7. Hourly data of CHP generation from 01.01.2016 to 31.10.2019

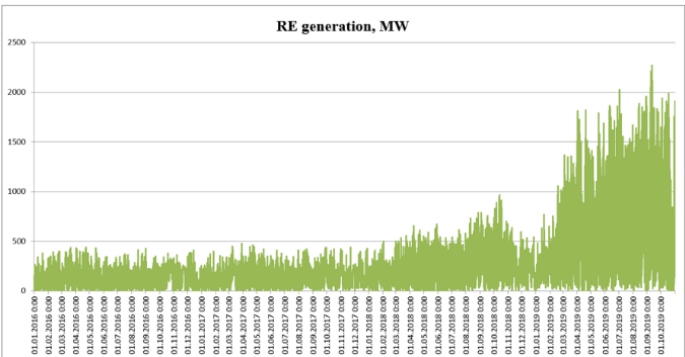


Fig. 8. Hourly data of RE generation from 01.01.2016 to 31.10.2019

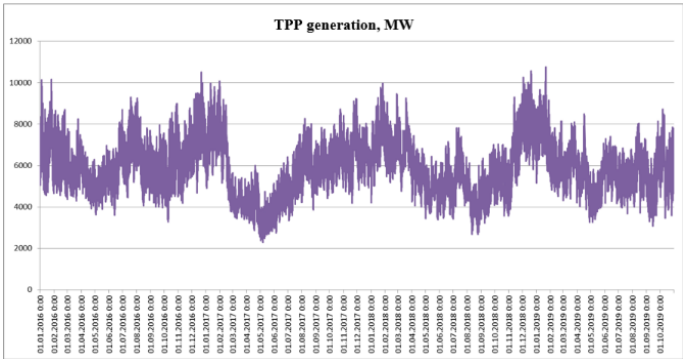


Fig. 9. Hourly data of TPP generation from 01.01.2016 to 31.10.2019

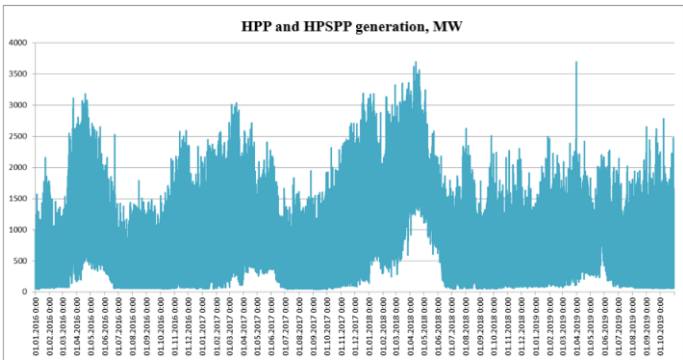


Fig. 10. Hourly data of HPP and HPSP generation from 01.01.2016 to 31.10.2019

An analysis of the hourly data for the period from 01.01.2016 to 31.10.2019 showed that an average of electricity generation per hour during the day was 17565 MW, 9452 MW of which belonged to NPP, 815 MW – CHP, 231 MW – RE, 5967 MW – TPP, 926 MW – HPP and HPSP and 174 MW – the pumping by HPSP. As percentage value this is as follows: 54.19% through NPP, 4.55% – CHP, 1.34% – RE, 33.84% – TPP, 5.14% – HPP and HPSP and 0.92 % – the pumping by HPSP.

According to the Law of Ukraine “On the electricity market” [1] fines will be imposed for failure to provide forecasts of renewable electricity generation or for failure to meet forecast of renewable electricity generation. However, the law does not define the mechanisms for collecting and analyzing data for forecasting generation and does not describe the requirements for the information base, type of data, algorithms and methodology for forecasting. This law does not indicate which infrastructure base should be for the necessary weather forecast, which is an extremely important and basic condition for solar and wind generation.

Also, the law does not specify information on the responsibility of the parties that must provide such data for generation forecasts, i.e. it must be directly electricity producers or third parties. There is no information on the permissible accuracy of these weather conditions for the possibility of forecasting, there are no guidelines for scheduling, monitoring, priority rules for generation distribution between market participants.

In the presence of a high share of solar power plants in the total capacity of renewable energy, there is no information on the infrastructure for ground-based cloud monitoring and simultaneous monitoring of cloud movement and density throughout Ukraine, local sunlight, which should be linked to a single information network, because this is a necessary condition for the most accurate short-term generation forecast and the ability to quickly balance.

For further research and forecasting of renewable electricity generation, statistical methods were used, which use real-time data to obtain statistically significant results. However, a large number of dependencies and meteorological processes are not accurately analyzed, because the priority is to establish a link between historical data on energy production and weather. The forecast of the possible amount of energy that will be produced is calculated based on such statistical relationships.

ARIMA models were considered first to predict the renewable electricity generation. These models provide one of the approaches to time series forecasting. In general, the model can be written as $ARIMA(p, d, q)$ model, where p is the order of the autoregressive part, d is the degree of first differencing involved, q is the order of the moving average part [20].

An autoregressive model of order p can be written as

$$y'(t) = a_0 + a_1 * y'(t - 1) + a_2 * y'(t - 2) + \dots + a_p * y'(t - p), \quad (1)$$

where $y'(t)$ is the differenced series (it may have been differenced more than once).

A stationary time series is one whose properties do not depend on the time at which the series is observed. But actually, almost all data are non-stationary, particularly financial and economic data, that is why one of the ways to make a non-stationary time series stationary is to compute the differences between consecutive observations. This is known as differencing and can be written as

$$y'(t) = y(t) - y(t - 1). \quad (2)$$

In addition, the differenced series can be white noise, which denotes as $\varepsilon(t)$. This leads to random walk models, which are widely used for non-stationary data:

$$y(t) = \varepsilon(t) + y(t - 1). \quad (3)$$

SARIMA models are models which include non-seasonal part of the ARIMA model and additional seasonal terms. This can be written as $\text{SARIMA}(p, d, q)(P, D, Q, m)$, where P is the seasonal order of the autoregressive part, D is the seasonal degree of first differencing involved, Q is the seasonal order of the moving average part, m is the number of observations per year.

An alternative approach TBATS [20] uses a combination of Fourier terms with an exponential smoothing state space model and a Box-Cox transformation which depend on the parameter ω , in a completely automated manner. As with any automated modelling framework, there may be cases where it gives poor results, but it can be a useful approach in some circumstances.

A TBATS model differs from dynamic harmonic regression in that the seasonality is allowed to change slowly over time in a TBATS model, while harmonic regression terms force the seasonal patterns to repeat periodically without changing. One drawback of TBATS models, however, is that they can be slow to estimate, especially with long time series.

The notation $y(\omega, t)$ is used to represent Box-Cox transformed observations with the parameter ω , where $y(t)$ is the observation at time t . It looks as follows

$$y(\omega, t) = \begin{cases} \frac{(y(t))^\omega - 1}{\omega}, & \omega \neq 0, \\ \log(y(t)), & \omega = 0, \end{cases} \quad (4a)$$

$$y(\omega, t) = l(t-1) + \phi b(t-1) + \sum_{i=1}^T s_i(t-m_i) + d(t), \quad (4b)$$

$$l(t) = l(t-1) + \phi b(t-1) + \alpha d(t), \quad (4c)$$

$$b(t) = \phi b(t-1) + \beta d(t), \quad (4d)$$

$$s_i(t) = s_i(t-m_i) + \gamma_i d(t), \quad (4e)$$

$$d(t) = \sum_{i=1}^p \phi_i d(t-1) + \sum_{j=1}^q \theta_j \varepsilon(t-j) + \varepsilon(t), \quad (4f)$$

where m_i , $i = 1, \dots, T$, denote the seasonal periods; T is amount of seasonality; $l(t)$ is the local level in period t ; $b(t)$ is the short-run trend in period t ; $s_i(t)$ represents the i^{th} seasonal component at time t ; $d(t)$ denotes an ARIMA process with ϕ and θ as parameters; and $\varepsilon(t)$ is a Gaussian white noise process with zero mean and constant variance σ^2 . The smoothing parameters are given by α , β and γ_i for $i = 1, \dots, T$ [21].

The following trigonometric representation introduces seasonal components based on Fourier series:

$$s_i(t) = \sum_{j=1}^{k_i} s_i(j, t), \quad (5)$$

$$s_i(j, t) = s_i(j, t-1) \cos \lambda_j^{(i)} + s_{*i}(j, t-1) \sin \lambda_j^{(i)} + \gamma_1^{(i)} d(t), \quad (6)$$

$$s_i(j, t) = -s_i(j, t-1) \sin \lambda_j^{(i)} + s_{*i}(j, t-1) \cos \lambda_j^{(i)} + \gamma_2^{(i)} d(t), \quad (7)$$

where $\gamma_1^{(i)}$ and $\gamma_2^{(i)}$ are smoothing parameters and $\lambda_j^{(i)} = 2\pi j/m_i$. The stochastic level of the i^{th} seasonal component is described by $s_i(j, t)$, $j = 1, \dots, k_i$, where each term is modeled using the Fourier series, the stochastic growth in the level of the i^{th} seasonal component, that is needed to describe the change in the seasonal component over time, is described by $s_{*i}(j, t)$. The number of harmonics required for the i^{th} seasonal component is denoted by k_i . It is equivalent to index seasonal approaches when $k_i = m_i/2$ for even values of m_i , and when $k_i = (m_i - 1)/2$ for odd values of m_i .

The automatic ARIMA forecasts are prone to large trend errors when there is a change in trend near the cutoff period and they fail to capture any seasonality. The exponential smoothing and seasonal naive forecasts capture weekly seasonality, but miss longer-term seasonality. All of the methods overreact to the end-of-year dip because they do not adequately model yearly seasonality.

When a forecast is poor, it is needed to have an ability to tune the parameters of the method to the problem at hand. Tuning these methods requires a thorough understanding of how the underlying time series models work. The first input parameters to automated ARIMA, for instance, are the maximum orders of the differencing, the auto-regressive components, and the moving average components. In general, it is difficult to adjust these orders to avoid the typical behavior of such models, because that is hard to scale.

In the article “Forecasting at Scale” [22] S. Taylor and B. Letham describe a time series forecasting model called Prophet and designed to handle the common features of business time series. Importantly, it is also designed to have intuitive parameters that can be adjusted without knowing the details of the underlying model. This is necessary for the analyst to effectively tune the model as described in Fig. 11.

Authors use a decomposable time series model with three main model components: trend, seasonality, and holidays. They are combined in the following equation:

$$y(t) = g(t) + s(t) + h(t) + \varepsilon(t). \quad (8)$$

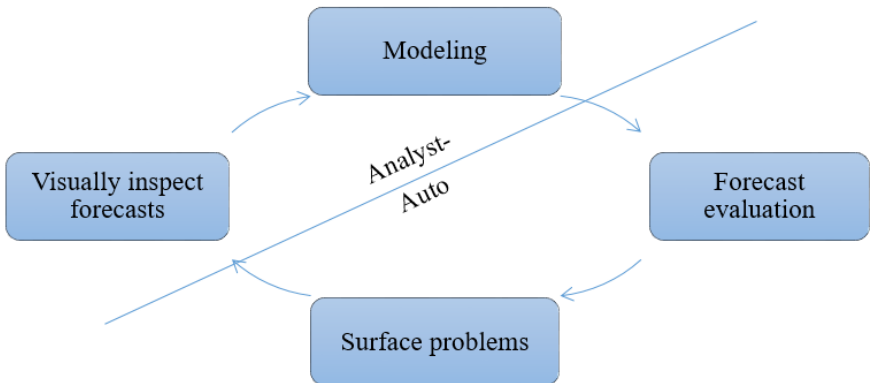


Fig. 11. Schematic view of the analyst-in-the-loop approach to forecasting at scale

Here $g(t)$ is the trend function which models non-periodic changes in the value of the time series, $s(t)$ represents periodic changes (e.g., weekly and yearly seasonality), and $h(t)$ represents the effects of holidays which occur on potentially irregular schedules over one or more days. The error term $\varepsilon(t)$ represents any idiosyncratic changes which are not accommodated by the model; later we will make the parametric assumption that $\varepsilon(t)$ is normally distributed.

This specification is similar to a generalized additive model (GAM) [23], a class of regression models with potentially non-linear smoothers applied to the regressors. Here we use only time as a regressor but possibly several linear and non-linear functions of time as components. Modeling seasonality as an additive component is the same approach taken by exponential smoothing. Multiplicative seasonality, where the seasonal effect is a factor that multiplies $g(t)$, can be accomplished through a log transform.

The GAM formulation has the advantage that it decomposes easily and accommodates new components as necessary, for instance when a new source of seasonality is identified. GAMs also fit very quickly, either using backfitting or L-BFGS so that the user can interactively change the model parameters.

For growth forecasting, the core component of the data generating process is a model for how the population has grown and how it is expected to continue growing. Modeling growth is often similar to

population growth in natural ecosystems, where there is nonlinear growth that saturates at a carrying capacity. This sort of growth is typically modeled using the logistic growth model, which in its most basic form is

$$g(t) = \frac{C}{1 + \exp(-k(t - m))}, \quad (9)$$

with C the carrying capacity, k the growth rate, and m an offset parameter.

There are two important aspects of growth that are not captured. First, the carrying capacity is not constant. Thus, the fixed capacity C was replaced with a time-varying capacity $C(t)$. Second, the growth rate is not constant.

Trend changes are incorporated in the growth model by explicitly defining changepoints where the growth rate is allowed to change. Suppose there are S changepoints at times s_j , $j = 1, \dots, S$. There is defined a vector of rate adjustments $\delta \in \mathbb{R}^S$, in which δ_j is the change in rate that occurs at time s_j . The rate at any time t is then the base rate k , plus all of the adjustments up to that point: $k + \sum_{j:t > s_j} \delta_j$. This is represented more cleanly by defining a vector $\mathbf{a}(t) \in \{0, 1\}^S$ such that

$$a_j(t) = \begin{cases} 1, & \text{if } t \geq s_j, \\ 0, & \text{otherwise.} \end{cases} \quad (10)$$

The rate at time t is then $k + \mathbf{a}(t)^T \delta$. When the rate k is adjusted, the offset parameter m must also be adjusted to connect the endpoints of the segments. The correct adjustment at changepoint j is easily computed as

$$\gamma_j = \left(s_j - m - \sum_{l < j} \gamma_l \right) \left(1 - \frac{k + \sum_{l < j} \delta_l}{k + \sum_{l \leq j} \delta_l} \right). \quad (11)$$

The piecewise logistic growth model is then

$$g(t) = \frac{C(t)}{1 + \exp\left(-(k + \mathbf{a}(t)^T \delta)(t - (m + \mathbf{a}(t)^T \boldsymbol{\gamma}))\right)}. \quad (12)$$

An important set of parameters in our model is $C(t)$, or the expected capacities of the system at any point in time. Analysts often have insight into market sizes and can set these accordingly.

For forecasting problems that do not exhibit saturating growth, a piece-wise constant rate of growth provides a parsimonious and often useful model. Here the trend model is

$$g(t) = (k + \mathbf{a}(t)^T \boldsymbol{\delta})t + (m + \mathbf{a}(t)^T \boldsymbol{\gamma}), \quad (13)$$

where, as before, k is the growth rate, $\boldsymbol{\delta}$ has the rate adjustments, m is the offset parameter, and $\boldsymbol{\gamma}_j$ is set to $-s_j \boldsymbol{\delta}_j$ to make the function continuous.

The changepoints s_j could be specified by the analyst using known dates of product launches and other growth-altering events, or may be automatically selected given a set of candidates.

Automatic selection can be done quite naturally with the formulation in (12) and (13) by putting a sparse prior on $\boldsymbol{\delta}$. Often a large number of changepoints are specified and the prior $\boldsymbol{\delta}_j \sim \text{Laplace}(0, \tau)$ is used [22]. The parameter τ directly controls the flexibility of the model in altering its rate. A sparse prior on the adjustments $\boldsymbol{\delta}$ has no impact on the primary growth rate k , so as τ goes to 0 the fit reduces to standard logistic or liner growth.

Time series often have multi-period seasonality. Seasonality models that are periodic functions of t must be specified to fit and forecast these effects. Fourier series are used to provide a flexible model of periodic effects. Let P be the regular period that the time series is expected to have (e.g. $P = 365.25$ for yearly data or $P = 7$ for weekly data, when the time variable is measured in days). It could approximate arbitrary smooth seasonal effects with [22]

$$s(t) = \sum_{n=1}^N \left(a_n \cos\left(\frac{2\pi nt}{P}\right) + b_n \sin\left(\frac{2\pi nt}{P}\right) \right). \quad (14)$$

Holidays and events provide large, somewhat predictable shocks to many business time series and often do not follow a periodic pattern, so their effects are not well modeled by a regular cycle. The impact of a particular holiday on the time series is often similar year after year, so it is important to take it into account in the forecast.

Incorporating this list of holidays into the model is made straightforward by assuming that the effects of holidays are independent. For each holiday i , let \mathbf{D}_i be the set of past and future dates for that holiday. An indicator function represents whether time t is during holiday i , and assign each holiday i a parameter $\kappa_i \in \boldsymbol{\kappa}$ which is the corresponding change in the forecast. This is done in a similar way as seasonality by generating a matrix of regressors

$$\mathbf{Z}(t) = [1(t \in \mathbf{D}_1), \dots, 1(t \in \mathbf{D}_L)] \quad (15)$$

and taking

$$h(t) = \mathbf{Z}(t)\boldsymbol{\kappa}. \quad (16)$$

As with seasonality, it is used a prior $\boldsymbol{\kappa} \sim \text{Normal}(0, \mathbf{v}^2)$.

It is often important to include effects for a window of days around a particular holiday. To account for that it is included additional parameters for the days surrounding the holiday, essentially treating each of the days in the window around the holiday as a holiday itself.

Finally, we propose the construction of autoregression's neural network (NNAR) [20] as a first baseline of deep learning model. This is a model of direct propagation with one hidden layer, where the values lag of the time series are given at the input. Basic form for non-seasonal (17) and seasonal (18) series:

$$\text{NNAR}(p, k), \quad (17)$$

$$\text{NNAR}(p, P, k)_{[m]}, \quad (18)$$

where p is the lag's order of the model's input data without taking into account seasonality ($y_{t-1}, y_{t-2}, \dots, y_{t-p}$); P is the lag order of the model input data taking into account the seasonality order m ($y_{t-m}, y_{t-2m}, \dots, y_{t-Pm}$); k is the number of neurons in the hidden layer.

For example, a NNAR(9, 5) model is a neural network with the last nine observations of a time series ($y_{t-1}, y_{t-2}, \dots, y_{t-9}$) used as inputs for forecasting the output y_t , and with five neurons in the hidden layer. A NNAR($p, 0$) model is equivalent to an ARIMA($p, 0, 0$) model, but without the restrictions on the parameters to ensure stationarity.

With seasonal data, it is useful to also add the last observed values from the same season as inputs. For example, an NNAR(3, 1, 2)_[12]

model has inputs ($y_{t-1}, y_{t-2}, y_{t-3}, y_{t-12}$), and two neurons in the hidden layer. More generally, an $NNAR(p, P, k)_{[m]}$ model has inputs ($y_{t-1}, y_{t-2}, \dots, y_{t-p}, y_{t-m}, y_{t-2m}, \dots, y_{t-Pm}$) and k neurons in the hidden layer. A $NNAR(p, P, 0)_{[m]}$ model is equivalent to an $ARIMA(p, 0, 0)(P, 0, 0)_{[m]}$ model but without the restrictions on the parameters that ensure stationarity.

The model is used iteratively for forecasting. All available data is used for the 1 step forward forecast. For two-step ahead forecasting at the input of the models a one-step forecast is given together with historical data. The process is continuing until achieved the horizon of the forecast.

NNAR it possible to learn a high order p model orders of magnitude faster than using least squares. Resulting weights are as interpretable, what makes this model more transparent than more complex deep learning models.

Model optimization is based on a selection of the model parameters by minimizing of the Akaike information criterion (AIC).

Results

The software package R was used to construct all next steps.

Hourly data of SPP and WPP electricity generation from 01.01.2016 to 29.10.2019 were taken from the Energy Map Web Portal of Open Data [24]. Visually assessing the dynamics of changes in generation indicators for this period, there is a sharp increase 01.01.2019 due to the implementation of new capacity in the IPS of Ukraine, which is why it was decided to use hourly data from 01.06.2018 (Fig. 12). In addition, the time series was divided into training and test samples. The test sample includes the actual generation indicators from 26.10.2019, 01:00:00 to 29.10.2019, 00:00:00. Accordingly, a forecast was made for this period and then its accuracy was measured.

Using the autocorrelation function (ACF), the partial autocorrelation function ($PACF$) and the Dickey-Fuller test, the time series was checked whether it is stationary – the current and future behavior of such time series coincides with the behavior that was in the past and changing the start of the countdown does not affect the properties of the time series.

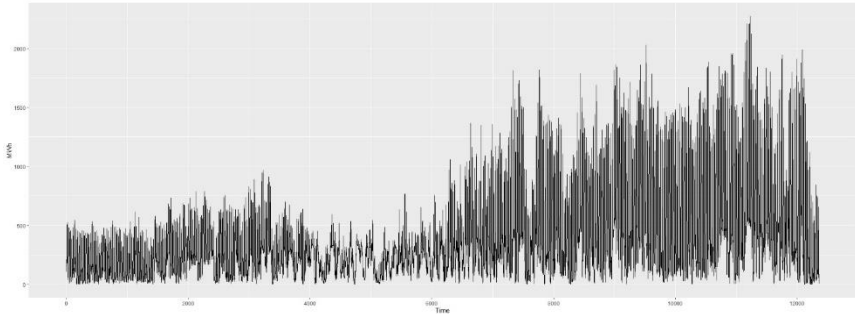


Fig. 12. The actual RE generation
for the period from 01.01.2019 to 29.10.2019

Figs. 13, 14 below shows obtained the *ACF* and *PACF* plots, where the dashed lines indicate the critical interval $\left[-\frac{2}{\sqrt{n}}; \frac{2}{\sqrt{n}}\right]$ within which the *ACF* and *PACF* values are considered to be non-zero.

Visual analysis of the *ACF* and *PACF* plots shows that the time series is not stationary, because there is a clear seasonality and outliers.

According to the Dickey-Fuller test, a time series is non-stationary if $t_{stat} > t_{crit}$. In this case, $t_{stat} = -7,2135$, while $t_{crit} = -2,58$. Therefore, according to this test, the time series is not stationary.

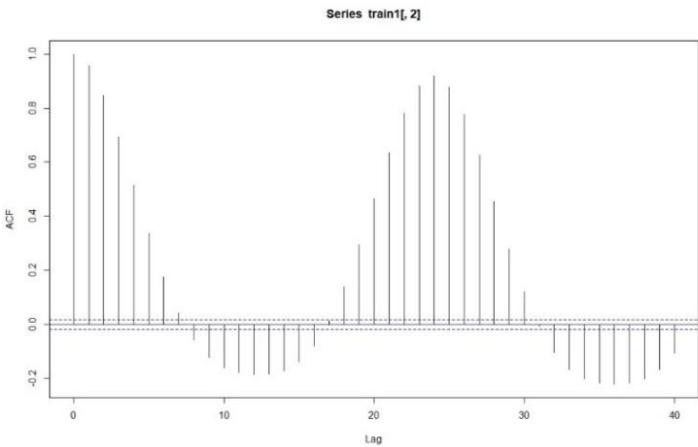


Fig. 13. The autocorrelation function (*ACF*)

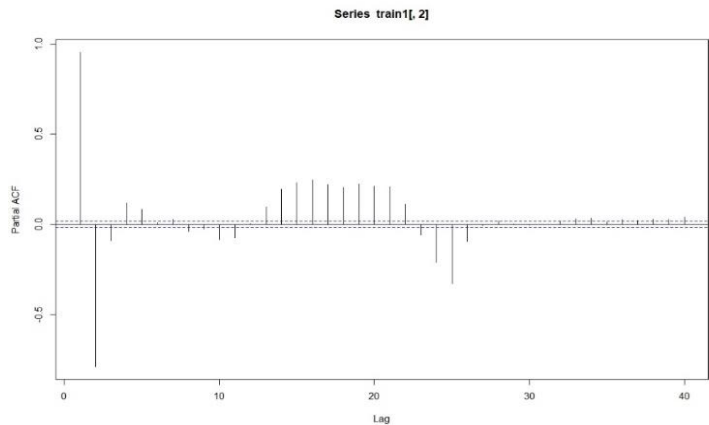


Fig. 14. The partial autocorrelation function (*PACF*)

The frequency of observations will be 24, because data that are observed have an hourly seasonality. Fig. 15 shows an additive decomposition of these data. There is the seasonality, which indicates that the ARIMA model should include additional seasonal terms.

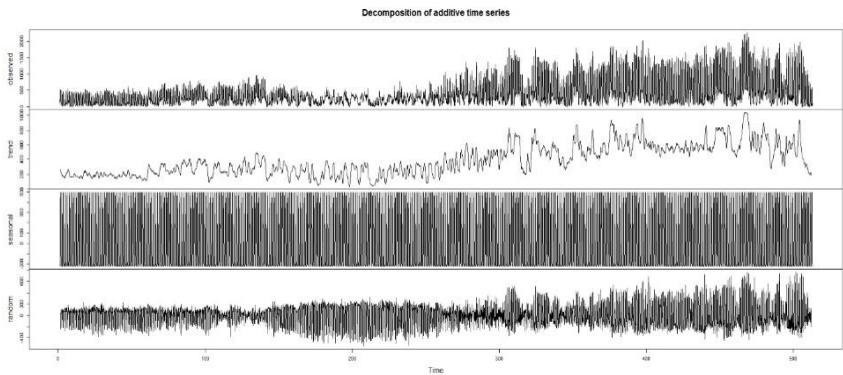


Fig. 15. The additive decomposition

Fig. 16 shows the results of the next 72-hour forecast with ARIMA (1) and TBATS (4b) models.

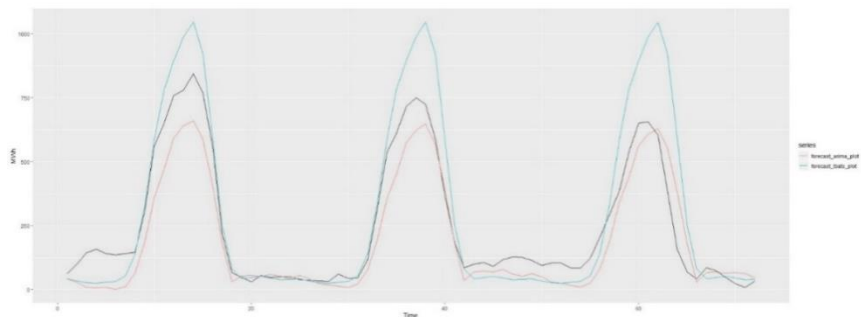


Fig. 16. Forecasts from an ARIMA and TBATS models

It can be concluded that the models caught the seasonality of the data, but the difference between the model and forecast values at peak load hours is quite large.

Visually, it could be assumed that if we take the average value of the ARIMA and TBATS models indicators, the result will be closer to the actual data. Fig. 17 shows that in this case such an assumption is relevant only for the first day of the forecast.

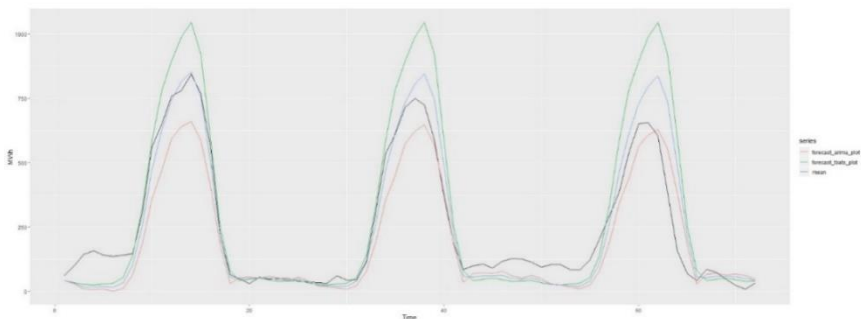


Fig. 17. Forecasts from an ARIMA and TBATS models and the average value of the ARIMA and TBATS models indicators

The most flexible model is the Prophet model (8), because it has intuitive parameters that can be adjusted and time as the main regressor. Modeling seasonality as an additive component uses the approach of exponential smoothing.

Several Prophet models with different parameters were built. In addition to the actual data of renewable energy generation in Ukraine, the hourly indicators of temperature, wind speed, number of sunshine hours for the period from 01.06.2018 to 26.10.2019 were used. The next 72-hour forecast was built using the combination of these indicators and seasonality (hourly, daily, weekly, monthly). It is important to note that during the construction of the models it turned out that the optimal period for the Prophet model is hourly data for the last 6-7 months (Fig. 18), because the behavior of the market at the beginning of its functioning is very different from current values, which introduces a bias in the value of forecasts.

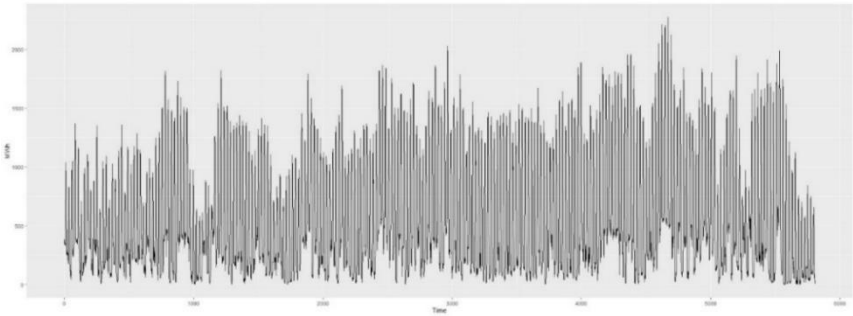


Fig. 18. The actual data of renewable energy generation in Ukraine for the period from 01.03.2019 to 29.10.2019

For all Prophet models we use cross-validation in the process of tuning their hyperparameters. We use grid search method for tuning potential changepoints, strength of the sparse prior, number of potential changepoints with different seasonality and features. Parameters are evaluated on *RMSE*:

$$RMSE = \sqrt{\frac{1}{n} \sum_{t=1}^n (\widehat{y(t)} - y(t))^2}. \quad (18)$$

The first version of the Prophet model (M0) is built on the actual generation indicators from 01.03.2019 with linear trend (13), potential changepoints in the first 94% of the time series, strength of the sparse prior 0.1, number of potential changepoints 35 and multiplicative daily and weekly seasonality (14).

The second version of the Prophet model (M1) is built on the same data as the previous one, but this time with linear trend, potential changepoints in the first 97% of the time series, strength of the sparse prior 0.05, number of potential changepoints 25 and multiplicative hourly, daily and weekly seasonality.

The third version of the Prophet model (M2) is built on the same data as the previous models, have linear trend, potential changepoints in the first 95% of the time series, strength of the sparse prior 0.08, and also multiplicative hourly, daily and weekly seasonality.

Since the renewable energy generation depends on the weather conditions, it is also advisable to include them into the model. The Prophet model allows to take into account additional regressors that affect the dependent variable.

The fourth version of the Prophet model (M3) is built on the previously generated dataset and takes into account additional weather conditions in the form of temperature, wind speed and number of sunshine hours, which were previously modeled using the Prophet model with linear trend, potential changepoints in the first 95% of the time series, strength of the sparse prior 0.9 and multiplicative hourly, daily and weekly seasonality.

The fifth version of the Prophet model (M4) contains the same parameters as the above model, but the forecast values of the generation are affected by additional regressors in the form of weather conditions, which were taken from the site of weather forecasting [25].

Fig. 19 shows the results of the next 72-hour forecast, which were obtained as a result of the construction of Prophet models.

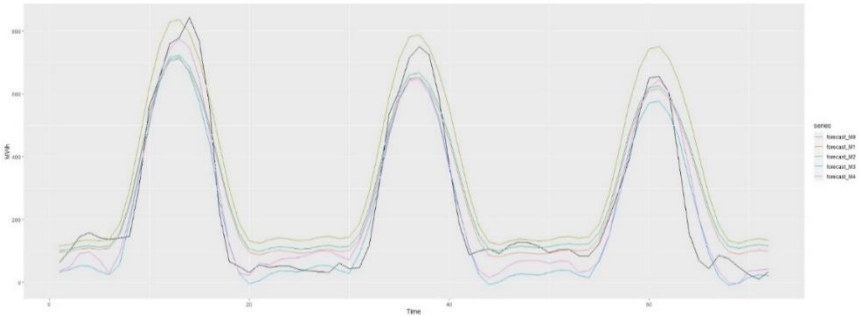


Fig. 19. Forecasts based on M0, M1, M2, M3, M4 models

In the last step there are build a series of NARR models where are choose three best. Depending on the time series components, we selected different settings for the model parameters by minimizing of the Akaike information criterion. The first model is the non-seasonal model NNAR(40, 20) that uses the last 40 lag's observations ($y_{t-1}, y_{t-2}, \dots, y_{t-40}$) with 20 neurons in the hidden layer. The second model is seasonal model NNAR(38, 1, 20)_[48] where to the inputs are fed $y_{t-1}, y_{t-2}, \dots, y_{t-38}$ and y_{t-48} with 20 neurons in the hidden layer. The third model is NNAR(36, 1, 18)_[48] ω which additionally uses the Box-Cox transformation with $\omega = 0.5$ (4a), has input layer from 36 lag observations $y_{t-1}, y_{t-2}, \dots, y_{t-36}$ plus one seasonal lag observation y_{t-48} and 18 neurons in the hidden layer.

Note that the selection of model parameters can also be optimized depending on the forecast horizon, that can significantly improve the efficiency of models, what will be the focus of our next study.

Fig. 20 shows the results of the next 72-hour forecast.

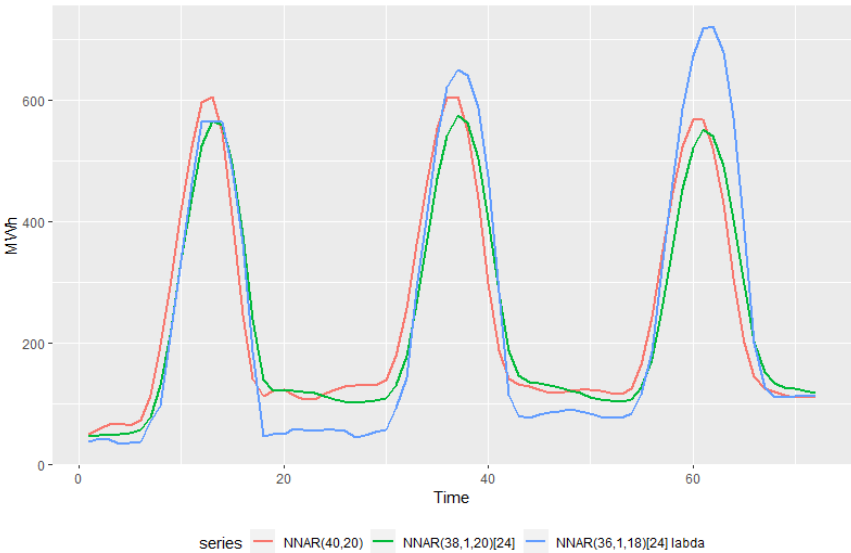


Fig. 20. Forecasts from NNAR models

The accuracy of the forecast values was checked using *RMSE* (18), *MAE* (19), *MAPE* (20):

$$MAE = \frac{1}{n} \sum_{t=1}^n |\widehat{y(t)} - y(t)|, \quad (19)$$

$$MAPE = \frac{1}{n} \sum_{t=1}^n \left| \frac{\widehat{y(t)} - y(t)}{y(t)} \right| \times 100\%. \quad (20)$$

The accuracy results for 6, 24, 48 and 72-hour forecast are shown in Table 2.

Table 2

ACCURACY OF FORECAST VALUES FOR THE PERIOD OF 6, 24, 48, 72 HOURS ACCORDING TO THE CONSTRUCTED MODELS

Model	RMSE	MAE	MAPE
the next 6-hour forecast			
Prophet (M0)	32,65	29,35	25%
Prophet (M1)	25,76	20,05	23%
Prophet (M2)	30,41	27,62	25%
Prophet (M3)	78,52	72,96	56%
Prophet (M4)	67,07	62,38	50%
ARIMA(2, 0, 1)(2, 1, 0) _[24]	117,24	107,73	81%
TBATS	99,63	92,11	70%
MEAN	108,39	99,92	75%
NNAR(40, 20)	66,53	61,13	46%
NNAR(38, 1, 20) _[48]	80,21	74,21	56%
NNAR(36, 1, 18) _[48] Ω	92,76	86,30	66%
the next 24-hour forecast			
Prophet (M0)	80,68	63,81	60%
Prophet (M1)	99,11	79,17	87%
Prophet (M2)	83,86	66,96	65%
Prophet (M3)	74,55	57,95	34%
Prophet (M4)	57,31	47,14	31%
ARIMA(2, 0, 1)(2, 1, 0) _[24]	117,62	95,96	44%
TBATS	94,58	68,97	32%
MEAN	64,68	45,74	31%
NNAR(40, 20)	141,01	106,57	65%
NNAR(38, 1, 20) _[48]	140,48	114,96	72%
NNAR(36, 1, 18) _[48] Ω	134,73	100,11	37%

Table 2 (continued)

Model	RMSE	MAE	MAPE
the next 48-hour forecast			
Prophet (M0)	76,16	61,50	66%
Prophet (M1)	103,55	84,42	98%
Prophet (M2)	80,18	64,85	72%
Prophet (M3)	66,92	54,19	40%
Prophet (M4)	61,45	53,19	47%
ARIMA(2, 0, 1)(2, 1, 0) _[24]	98,98	76,22	39%
TBATS	114,69	78,18	33%
MEAN	62,59	45,46	30%
NNAR(40, 20)	118,40	90,93	76%
NNAR(38, 1, 20) _[48]	119,03	95,92	71%
NNAR(36, 1, 18) _[48] Ω	103,37	71,89	33%
the next 72-hour forecast			
Prophet (M0)	86,70	63,69	85%
Prophet (M1)	121,29	96,51	124%
Prophet (M2)	89,38	68,00	93%
Prophet (M3)	67,03	53,81	48%
Prophet (M4)	63,85	52,39	52%
ARIMA(2, 0, 1)(2, 1, 0) _[24]	95,09	74,21	51%
TBATS	151,42	98,79	50%
MEAN	89,94	60,76	45%
NNAR(40, 20)	104,81	80,53	88%
NNAR(38, 1, 20) _[48]	112,76	88,73	91%
NNAR(36, 1, 18) _[48] Ω	115,27	76,64	66%

Thus, it can be concluded that weather conditions definitely need to be involved in the model, as well as seasonality. This allows to predict an increase or decrease in renewable energy generation and respond in a timely manner to balance. However, in this case the weather conditions help to optimize the model only partially, as the actual renewable energy generation data are general values, and the weather conditions are averaged.

The most important forecast error for electricity generation is the difference between the prediction capacity and the actual capacity of electricity generated. This error is expressed by the *MAE*. According

to this indicator for the operational forecast (6 hours) the best models are Prophet (M1) with hourly seasonality – 20.05 and Prophet (M2) with hourly, daily and weekly seasonality – 27.62. For the short-term forecast (24 hours) and the 48-hour forecast, the most accurate models are Prophet (M4) with hourly, daily, weekly seasonality and forecast weather conditions, which were taken from the weather forecast site [25], and modeled independently – 47.14 and 57.95, respectively, and also the average value MEAN of ARIMA and TBATS models – 45.74 and 45.46, respectively. According to this indicator for the medium-term forecast (72 hours) the most accurate models are Prophet (M3, M4) with hourly, daily, weekly seasonality and weather conditions – 52.39 and 53.81, respectively.

According to the *RMSE* for the operational forecast (6 hours), the best models are Prophet (M1) with hourly seasonality – 25.76 and Prophet (M2) with hourly, daily and weekly seasonality – 30.41. For the 24-hour and 48-hour forecast, the most accurate models are Prophet (M4) with hourly, daily, weekly seasonality and forecast weather conditions, which were taken from the source [25] – 57.31 and 61.45, respectively, and the average values of ARIMA and TBATS models – 64.68 and 62.59, respectively. For the medium-term forecast (72 hours), the most accurate models are Prophet (M3, M4) with hourly, daily, weekly seasonality and weather conditions – 63.85 and 67.03, respectively.

According to the *MAPE* for the operational forecast (6 hours), the best models are Prophet (M1) with hourly seasonality – 22.53% and Prophet (M2) with hourly, daily and weekly seasonality – 24.70%. For the short-term forecast (24 hours) in this case the most accurate are the average values of ARIMA and TBATS models – 30.86% and Prophet (M3, M4) with hourly, daily, weekly seasonality and weather conditions – 30.99% and 33.95%, respectively. For the 48-hour forecast the most accurate models are the ARIMA, TBATS models and their average value (MEAN) – 38.95%, 33.12% and 29.53%, respectively. For the medium-term forecast (72 hours) the most accurate models are Prophet (M3) with hourly, daily, weekly seasonality and weather conditions – 47.80% and average value of ARIMA and TBATS models – 45.23%.

Fig. 21 shows the results of the next 6-hour forecast. It can be clearly seen that in comparison with others, the Prophet model (M4)

with hourly, daily, weekly seasonality and forecast weather conditions, which were taken from the weather forecast site [25], is the only model that caught a complex trend, despite the large deviations. It can be concluded that an accurate forecast of weather conditions is an important component for effective forecasting of renewable energy generation.

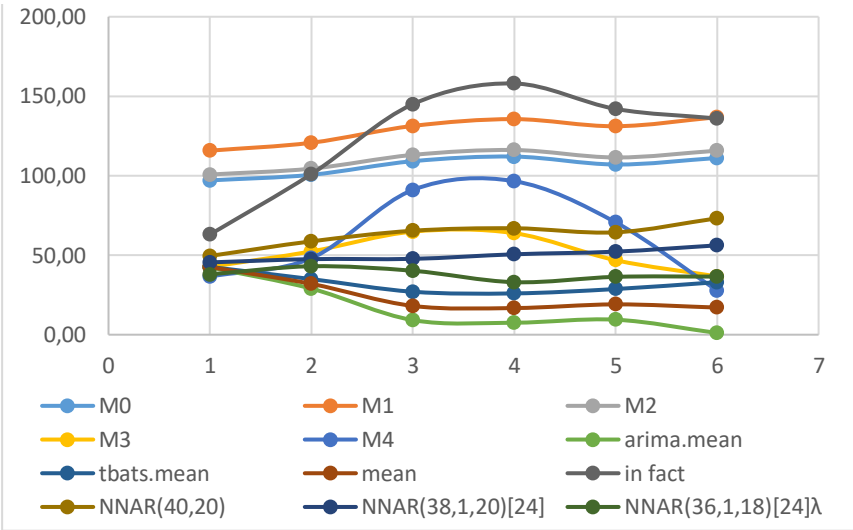


Fig. 21. Actual data and the results of the next 6-hour forecast, MW

Fig. 22 shows the results of the next 24-hour forecast. Here we can see that all the forecast values of Prophet models quite clearly describe the trend in peak load hours, namely in the period from 9 hours to 16 hours.

Fig. 23 shows that for the next 48-hour forecast Prophet models also describe the time series quite clearly at peak load hours. In addition, these models caught the general trend of decreasing generation, as it directly depends on weather conditions. During the period from 42 hours to 48 hours, the ARIMA model was the only one to caught the trend of the time series, despite the deviation in the forecast values of more than 15%.

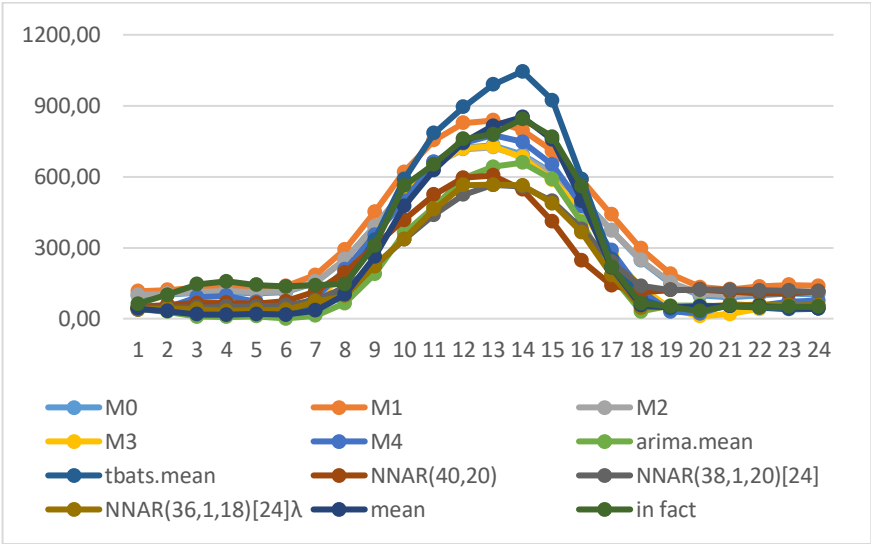


Fig. 22. Actual data and the results of the next 24-hour forecast, MW

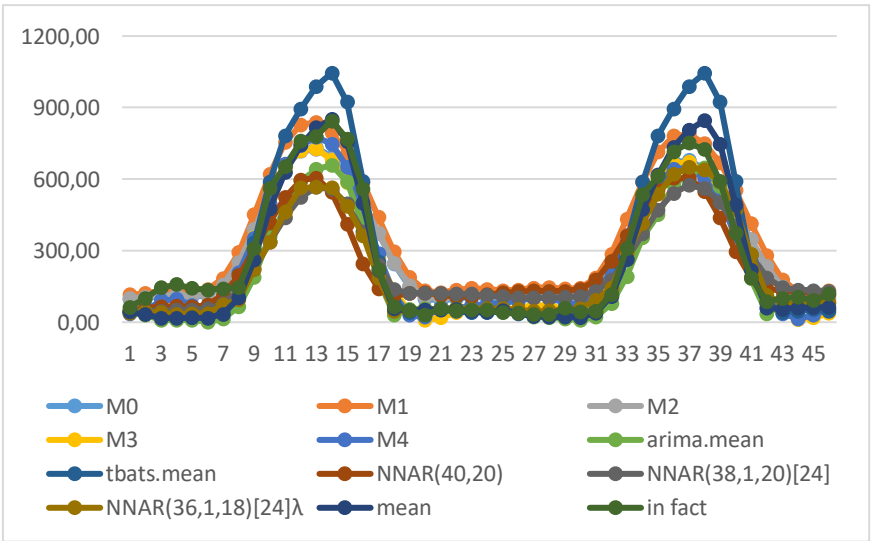


Fig. 23. Actual data and the results of the next 48-hour forecast, MW

Fig. 24 shows that for the next 72 hours all forecast values of the models, except the TBATS, the Prophet (M1) and the average value of ARIMA and TBATS, caught the seasonal component of time series.

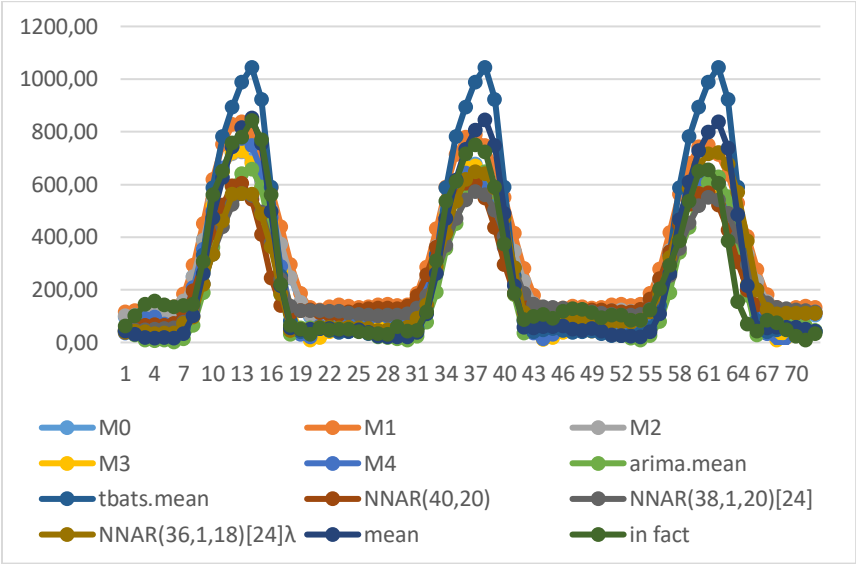


Fig. 24. Actual data and the results of the next 72-hour forecast, MW

Unfortunately, from 00:00 to 09:00, the deviations of almost all forecast values exceed the permissible limits, which indicates the need for effective and accurate weather forecasts, especially for wind speeds.

Accordingly, in all hours where there are deviations outside the allowable limits, it will be necessary to reimburse the cost of adjusting the imbalance.

Therefore, to obtain the most accurate calculations for the operational forecast it is important to take into account hourly, daily and weekly seasonality, for short-term and medium-term forecast it is necessary to involve additional regressors, including weather conditions, since their inaccuracy has a great impact on the models.

Conclusion

The process of entering into the pan-European energy market has led to the formation of a new electricity market in Ukraine, which started to operate on July 1, 2019. This necessitates more extensive research, analysis and forecasting of electricity production from renewable sources.

In this study, the forecasting of renewable electricity generation in Ukraine was carried out according to the seasonal ARIMA, TBATS, Prophet models and using the software package R. Most attention is paid to models such as Prophet, because it is very flexible and has intuitive parameters that can be adjusted. Operative (6 hours), short-term (24 hours), medium-term (48 and 72 hours) forecasts were built.

The MAE criterion shows that the best models for the operational forecast are Prophet model with hourly seasonality – 20.05 and Prophet model with hourly, daily and weekly seasonality – 27.62. For the short-term forecast, the most accurate models are Prophet with hourly, daily, weekly seasonality and forecast weather conditions, which were taken from the site of the weather forecast – 47.14 and 57.95 respectively and the average values of ARIMA and TBATS models – 45.74 and 45.46, respectively. According to this indicator, for the medium-term forecast, the most accurate models are Prophet models with hourly, daily, weekly seasonality and weather conditions (both taken from the side and simulated by hand) – 52.39% and 53.81%, respectively.

Proposed approach has demonstrated sufficient efficiency for Ukraine and can be used as a basis for forecasting the production of electricity from renewable sources. In the future, we plan to focus on an in-depth study of more complex deep learning models in renewable electricity generation forecasting problems, as well as on new methods for fitting hyperparameters.

References

1. Verkhovna Rada. (2017). *Pro rynek elektrychnoi enerhii [On the electricity market]* (Law of Ukraine 2019-VIII). Retrieved February 7, 2021, from <https://zakon.rada.gov.ua/laws/show/2019-19> [in Ukrainian]

2. Verkhovna Rada. (2003). *Pro alternatyvni dzhherela enerhii [On Alternative Energy Sources]* (Law of Ukraine 555-IV). Retrieved February 7, 2021, from <https://zakon.rada.gov.ua/laws/show/555-15> [in Ukrainian]
3. Verkhovna Rada. (2005). *Pro kombinovane vyrobnytstvo teplovoi ta elektrychnoi enerhii (koheneratsiiu) ta vykorystannia skydnoho enerhopotentsialu [On Combined Heat and Power (Cogeneration) and Waste Energy Potential]* (Law of Ukraine 2509-IV). Retrieved February 7, 2021, from <https://zakon.rada.gov.ua/laws/show/2509-15> [in Ukrainian]
4. Verkhovna Rada. (2016). *Pro Natsionalnu komisiuu, shcho zdiisniue derzhavne rehuliuвання u sferakh enerhetyky ta komunalnykh posluh [On National Commission for State Regulation of Energy and Utilities]* (Law of Ukraine 1540-VIII). Retrieved February 7, 2021, from <https://zakon.rada.gov.ua/laws/show/1540-19> [in Ukrainian]
5. Verkhovna Rada. (2000). *Pro pryrodni monopolii [On natural monopolies]* (Law of Ukraine 1682-III). Retrieved February 7, 2021, from <https://zakon.rada.gov.ua/laws/show/1682-14> [in Ukrainian]
6. Verkhovna Rada. (2001). *Pro zakhyst ekonomichnoi konkurentsii [On protection of economic competition]* (Law of Ukraine 2210-III). Retrieved February 7, 2021, from <https://zakon.rada.gov.ua/laws/show/2210-14> [in Ukrainian]
7. Verkhovna Rada. (1991). *Pro okhoronu navkolyshnoho pryrodnoho seredovyscha [On environmental protection]* (Law of Ukraine 1264-XII). Retrieved February 7, 2021, from <https://zakon.rada.gov.ua/laws/show/1264-12> [in Ukrainian]
8. Hong, T., Pinson, P., Wang, Y., Weron, R., Yang D., & Zareipour, H. (2020). Energy Forecasting: A Review and Outlook. *IEEE Open Access Journal of Power and Energy*, 7, 376-388. <https://doi.org/10.1109/OAJPE.2020.3029979>
9. Harrou, F., & Sun, Y. (2020). *Advanced Statistical Modeling, Forecasting, and Fault Detection in Renewable Energy Systems*. IntechOpen. <http://doi.org/10.5772/intechopen.85999>
10. Bangert, P. (2021). *Machine Learning and Data Science in the Power Generation Industry: Best Practices, Tools, and Case Studies*. Elsevier. <https://doi.org/10.1016/C2019-0-00440-2>
11. Liu, H., & Chen, C. (2019). Data processing strategies in wind energy forecasting models and applications: A comprehensive review. *Applied Energy*, 249, 392–408. <https://doi.org/10.1016/j.apenergy.2019.04.188>

12. Qian, Z., Pei, Y., Zareipour, H., & Chen, N. (2019). A review and discussion of decomposition-based hybrid models for wind energy forecasting applications. *Applied Energy*, 235, 939–953. <https://doi.org/10.1016/j.apenergy.2018.10.080>
13. Blaga, R., Sabadus, A., Stefu, N., Dughir, C., Paulescu, M., & Badescu, V. (2019). A current perspective on the accuracy of incoming solar energy forecasting. *Progress in Energy and Combustion Science*, 70, 119–144. <https://doi.org/10.1016/j.peccs.2018.10.003>
14. Liu, H., Chen, C., Lv, X., Wu, X., & Liu, M. (2019). Deterministic wind energy forecasting: A review of intelligent predictors and auxiliary methods. *Energy Conversion and Management*, 195, 328–345. <https://doi.org/10.1016/j.enconman.2019.05.020>
15. Mashlakov, A., Kuronen, T., Lensu, L., Kaarna, A., & Honkapuro, S. (2021). Assessing the performance of deep learning models for multivariate probabilistic energy forecasting. *Applied Energy*, 285, Article 116405. <https://doi.org/10.1016/j.apenergy.2020.116405>
16. Rodríguez, F., Fleetwood, A., Galarza, A., & Fontán, L. (2018). Predicting solar energy generation through artificial neural networks using weather forecasts for microgrid control. *Renewable Energy*, 126, 855–864. <https://doi.org/10.1016/j.renene.2018.03.070>
17. Zhou, H., Zhang, Y., Yang, L., Liu, Q., Yan, K., & Du, Y. (2019). Short-Term Photovoltaic Power Forecasting Based on Long Short Term Memory Neural Network and Attention Mechanism. *IEEE Access*, 7, 78063–78074. <https://doi.org/10.1109/access.2019.2923006>
18. Ministry of Energy of Ukraine. (2017). *Enerhetychna stratehiia Ukrainy na period do 2035 roku [Energy Strategy of Ukraine up to 2035]* (Order of the Cabinet of Ministers of Ukraine of August 18, 2017 No. 605). http://mpe.kmu.gov.ua/minugol/control/uk/publish/article?art_id=245239564&cat_id=245239555 [in Ukrainian]
19. National Power Company Ukrenergo. (2020). *Vstanovlena potuzhnist enerhosystemy Ukrainy [Installed capacity of the power system of Ukraine]*. Retrieved January 21, 2020, from <https://ua.energy/vstanovlena-potuzhnist-energosystemy-ukrayiny/> [in Ukrainian]
20. Hyndman, R.J., & Athanasopoulos, G. (2018). *Forecasting: principles and practice* (2nd ed.). OTexts. <https://otexts.org/fpp2/>
21. De Livera, A. M., Hyndman, R. J., & Snyder, R. D. (2011). Forecasting time series with complex seasonal patterns using exponential smoothing. *Journal of the American Statistical Association*, 106(496), 1513–1527. <https://doi.org/10.1198/jasa.2011.tm09771>

22. Taylor, S. J., & Letham, B. (2017). Forecasting at Scale. *PeerJ Preprints*, 5, Article e3190v2. <https://doi.org/10.7287/peerj.preprints.3190v2>
23. Hastie, T., & Tibshirani, R. (1987). Generalized Additive Models: Some Applications. *Journal of the American Statistical Association*, 82(398), 371–386. <https://doi.org/10.2307/2289439>
24. Energy Map. (2016-2019). *Hourly power balance of IPS of Ukraine* [Data set]. Retrieved January 21, 2020, from <https://map.ua-energy.org/en/resources/8998f2ed-379f-4fa9-9076-88782b32ee4f/>
25. Ukrainian Hydrometeorological Center. (2021). *Weather archive* [Data set]. Retrieved February 7, 2021, from https://meteo.gov.ua/en/33345/climate/climate_stations

The article was submitted on 2021, March 24